Stress Corrosion Cracking of Candidate Alloys for the Supercritical Water Reactor Concept

Annual Report

University of Michigan

Gary S. Was, PI
Sebastien Teysseyre
Qunjia Peng

Summary

The supercritical water test facility for conducting constant extension rate tensile (CERT) and crack growth rate (CGR) experiments on neutron-irradiated materials is complete, benchmarked and has undergone a dry run. It is now qualified to accept neutron-irradiated materials, and a plan is in place for the receipt and testing of neutron-irradiated tensile samples in FY2006. This facility is now the only facility in the world that has the capability to conduct SCC tests on neutron-irradiated samples in supercritical water in support of the SCWR. This report covers the activity of our program over FY2005 by milestone. In particular, it provides a description of the SCW system for SCC testing of neutron-irradiated samples, the system testing procedure, test results, benchmark test and dry run and the NRC license at the University of Michigan for accepting radioactive samples.

September 2005

University of Michigan
Ann Arbor, MI 48109-2104

Stress Corrosion Cracking of Candidate Alloys for the Supercritical Water Reactor Concept

Annual Report

1. Completion of the Autoclave and SCC Facility

The multi-sample test facility for conducting CERT and CGR tests on neutron-irradiated materials utilizes two laboratories in the Phoenix Memorial Laboratory at the University of Michigan. They are the Irradiated Materials Testing Laboratory (IMTL) and hot cell #1, which together comprise the Irradiated Materials Testing Complex (IMTC). IMTL is a 1000 sq ft room (#1059) in which CERT and CGR experiments are conducted. Hot cell #1 is used for specimen loading, autoclave closure and pressure testing and sample unloading after test completion. It is also used for post-test SEM analysis of fracture and gage sections. The schematic in Fig. 1 shows the two-laboratory complex.

1.1 Description of the SCC facility

The SCC facility provides the means to perform stress corrosion cracking experiments on irradiated samples in pure supercritical water, up to 30 MPa of pressure and 600ºC, in a controlled, refreshed environment. The environmental control allows the conductivity to be maintained below 0.1 μS/cm and the dissolved oxygen content below 10 ppb. Constant strain rate, constant load and constant K can be applied to the specimens.

The testing facility consists of a closed loop, flowing water system. The water chemistry is first prepared and controlled in the water board, then the water is pressurized and heated up to test condition before it flows into the autoclave. It then flows back from the autoclave and is cooled down to room temperature through two heat exchangers before it reaches the water board where the pressure is reduced and the water chemistry is measured. All of the main parameters affecting the test such as temperature, pressure, dissolved oxygen content, conductivity, applied load and sample displacement are continuously monitored and recorded. A schematic of the system is provided in Fig. 2 and the assembled system is shown in Fig. 3.

Complete description of the SCC facility will be provided in 3 parts: the water board, the preheating-cooling unit, and the loading unit. The water board and the preheating-cooling unit are permanently installed in IMTL whereas the loading unit can be disconnected. Then additional information about the laboratory related to safety and regulation will be presented. Finally, the flange tensioning system and the DCPD unit will be presented.

1.1.1 Water board.

The water board is the part of the unit where water is stored, the water chemistry is controlled and measured, and where the system is brought up to pressure. A schematic of the water board is shown Fig. 2. The ultra pure water provided by the distillation unit of the laboratory is stored in two glass columns. Both columns are connected to a recirculation loop that passes the outlet water through on an ion exchange column. Gas is bubbled in the columns and an over pressure is be applied in order to control the dissolved gas content (dissolved oxygen for the current application) of the water. As the primary column contains the water to be used for the experiment, a conductivity meter and an oxygen meter are installed in the recirculation loop to permit continuous monitoring of the conductivity and dissolved oxygen content. The secondary column refills the primary column.

A high-pressure pump delivers the water from the primary column to the vessel through the preheater and controls the flow rate for the experiment. The pump is a Prep 250 provided from Lab Alliance that can deliver a flow rate up to 250ml/min and maintain a pressure up to 5000 psi.

Water returning from the vessel passes through the preheating-cooling unit and then returns to the water board. It then goes through a 0.5 μm filter, a back pressure regulator (BPR) and then an ion exchange column. The part of the loop between the pump and the BPR (preheating-cooling unit and autoclave) is at the pressure set by activating the BPR and is measured by a pressure gage and two pressure transducers (located both at the inlet line and the outlet line). After the BPR, the water is at low pressure and flows through a conductivity meter and an oxygen meter before it goes back to the primary column.

1.1.2 Preheating-cooling unit

The water needs to be brought as close as possible to the testing condition before it flows to the vessel to assure a stable and uniform environment inside the autoclave. Therefore the pressurized water that comes from the water board needs to be heated close to the target test temperature. This is achieved by flowing the inlet water through a regenerative heat exchanger that takes its heat from the water leaving the vessel. After leaving the heat exchanger, the inlet water flows through preheater, consisting of a coil heated by 4 heating cords controlled by 2 temperature controllers. The preheater unit (heat exchanger plus heated coil) is enclosed in a 16”x9”x14” ceramic insulating box. The water temperature is recorded at the exit of the heat exchanger and at the exit of the preheater (before the water flows in the vessel). Upon leaving the autoclave, the outlet water first runs through the regenerative heat exchanger described previously where heat is transferred to the inlet water. The water temperature is brought to room temperature by flowing the water though a non-regenerative heat exchanger (chiller) before it returns to the water board.

1.1.3 Loading unit

The loading unit is composed by the autoclave, the servo motor that applies load or strain to the samples and the load frame that support the assembly. The autoclave consists of a head assembly and a body. There are two heads; one for CERT tests and one for CGR tests. The CERT head allows the loading of four samples at a time. The load is applied to each sample through a 3/16" diameter pull rod. The pull rod diameter was chosen as a compromise between the need to assure sufficient stiffness of the loading jig and to limit the loading of the samples due to the internal pressure. A thermocouple measures the temperature of the environment next to the samples. The head has two openings for future electrochemical measurements.

The CGR head uses a ¼" pull rod. Besides a thermocouple port, this head has openings to feed the leads needed for DCPD and, as for the CERT head, two extra openings were added. Once the autoclave is closed, heater bands are installed around the body to control the vessel temperature, and insulation is applied to minimize heat loss.

The servo motor and controller provided by Axis Analytical can be used in constant strain, constant load, constant K and fatigue mode. The motor is permanently fixed to the load frame and is located directly beneath the vessel. The motor and the pull rod are connected via load cells that permit the measurement of the load applied on each sample. For CERT tests, an LVDT is installed to measure the displacement rate. The autoclave and the motor are installed on a load frame that also is designed to carry the load of a shield when radioactive samples are used. The loading unit can be disconnected from the water loop to be moved into and out of the hotcell.

1.1.4 Safety-regulation considerations

The facility has several safety features included in this design due to the high pressure, high temperature capability and the potential for radioactive contamination. There are three systems that set the limit on the attainable pressure. First the pump is configured in a way that prevents the pump from operating above a set maximum pressure. Second, a relief valve is installed after the pump with an adjustable pressure setting. Finally, a rupture disk is installed in the outlet line after the preheater-cooling unit and just before the water enters the water board on return from the autocalve. This safety feature instantaneously dumps the hot water into a sparge tank. Each temperature controller is equipped with an alarm that shuts off the power if the temperature exceeds a set value.

The system was designed so that the operator has access to each control point of the system, regardless of proximity to the system. This was achieved by building a control panel outside of the closed area where the facility is located as shown in Fig.3. In addition to these safety features, the Labview monitoring software is interfaced with a paging system so that if the temperature or pressure exceed set limit values, the operator receives a page notifying him of the status of the system. This paging system keeps the operator in touch with the facility operation 24 hours a day.

Regulations prohibit the release of potentially contaminated liquid to the environment. An uncontrolled release of water could occur from two points in the system: the exit of the rupture disk, and the coolant line of the non-regenerative heat exchanger. As described previously, the exit of the rupture disk is connected to a sparge tank that stores the water in IMTL. The non-regenerative heat exchanger is connected to a closed-loop chiller in which heat is rejected to the air. So any leakage will be confined within the system.

1.1.5 Flange tensioning system

Since the crucial step of closing and sealing the vessel must be conducted remotely, in the hotcell, we acquired a custom-made flange tensioning system. The flange tensioner is a device that hydraulically loads the flange by pulling against the studs. The tensioner consists of a segmented annular ring with a number of internally connected hydraulic chambers. Only one connection is necessary for each segment to pressurize the rams simultaneously, and sealing can be achieved in a single operation. This is to be compared with the conventional method of sealing that requires tightening each bold individually, in a specified patter (star pattern) in small increments of load. Such a process would require each bolt to be tightened a minimum of 6 times for a total of at least 72 operations to seal the autoclave. Further, the application of uniform pressure around the entire seal provides much more reproducibility and uniformity and will greatly enhance success with achieving a water-tight seal that is so important for such high pressures. This tool makes the sealing process of the autoclave in the hotcell faster, easier and more reliable than conventional methods.

1.1.6 Electronic equipment for DCPD

The SCC facility provides the means for constant K loading in crack growth rate mode. To assess the crack propagation during the test and apply the appropriate load, a direct current potential drop (DCPD) system was built . The DCPD unit consists in a highly stable power supply, a nano-voltmeter, a data acquisition switch unit from Agilent and a reverse current unit. The control of the current, the calculation of the crack depth, the motor control and the data monitoring is performed by a desktop computer. The operation of the DCPD system is described in more detail in section 3.2 of the report.

1.2 Testing of the SCC facility

Following completion of the system assembly, a demonstration test was conducted to ensure that the system was leak-tight and capable of straining samples in a supercritical water environment. To test the operation of the facility, a CERT test was performed on four “dummy” samples. The target pressure and temperature were achieved and four dummy samples were strained at a rate of 10^{-6} s^{-1}. The test was stopped after the first sample failed. The test conditions are summarized Table 1.

This test was also used to begin cleaning and conditioning the system in order to be able to assure good water chemistry control in future tests. As a result, conductivity and oxygen content were not controlled. Figure 4 show the temperature and pressure history for the test. The system behaved well and the check-out test was successfully completed.

Table 1. Conditions used for the demonstration test of the hot SCW facility

Pressure	25.5 MPa (3700 psi)
Temperature	500°C
Samples	4 tensile samples: • Prestrained 304L • cold worked alloy 600 • Inconel 625 • Inconel 690
Strain rate	10^{-6} s^{-1}

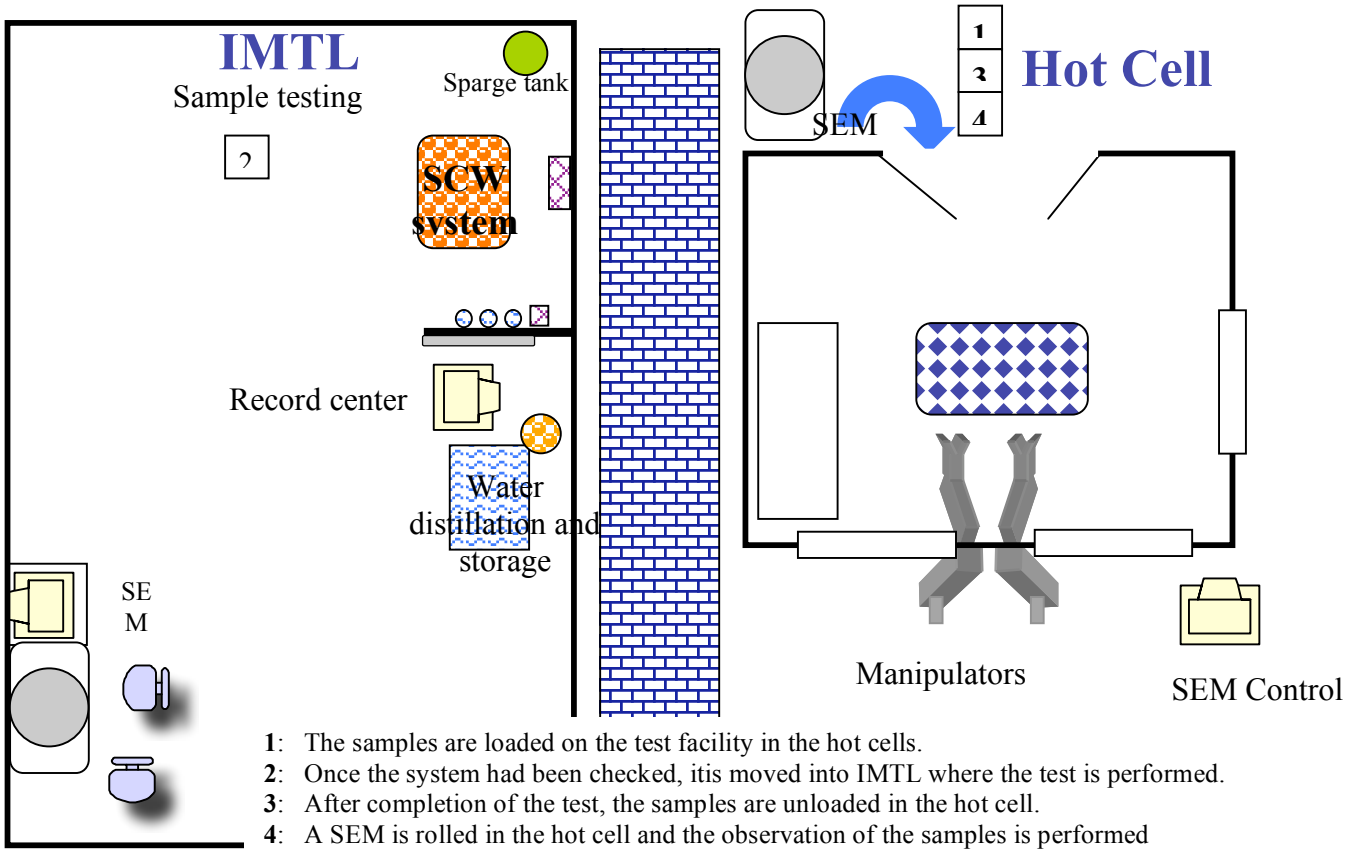

Figure 1. Schematic of the Irradiated Materials Testing Facility, consisting of the Irradiated Materials Testing Laboratory and Hot Cell #1, and the arrangement of instrumentation for conducting CERT and CGR tests and post-test fractographic analysis on neutron-irradiated materials via SEM.

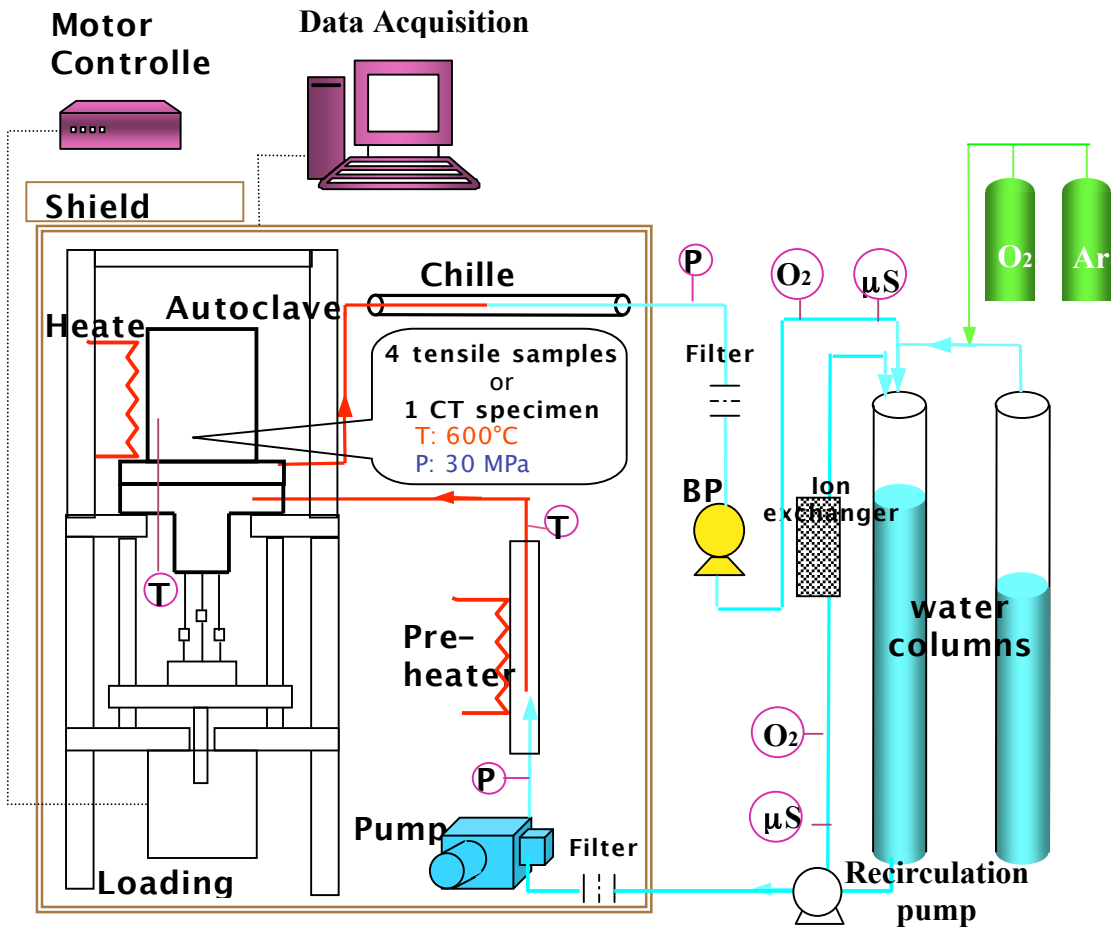

Figure 2. Overall schematic of the water loop for the SCW autoclave system in the Irradiated Materials Testing Laboratory.

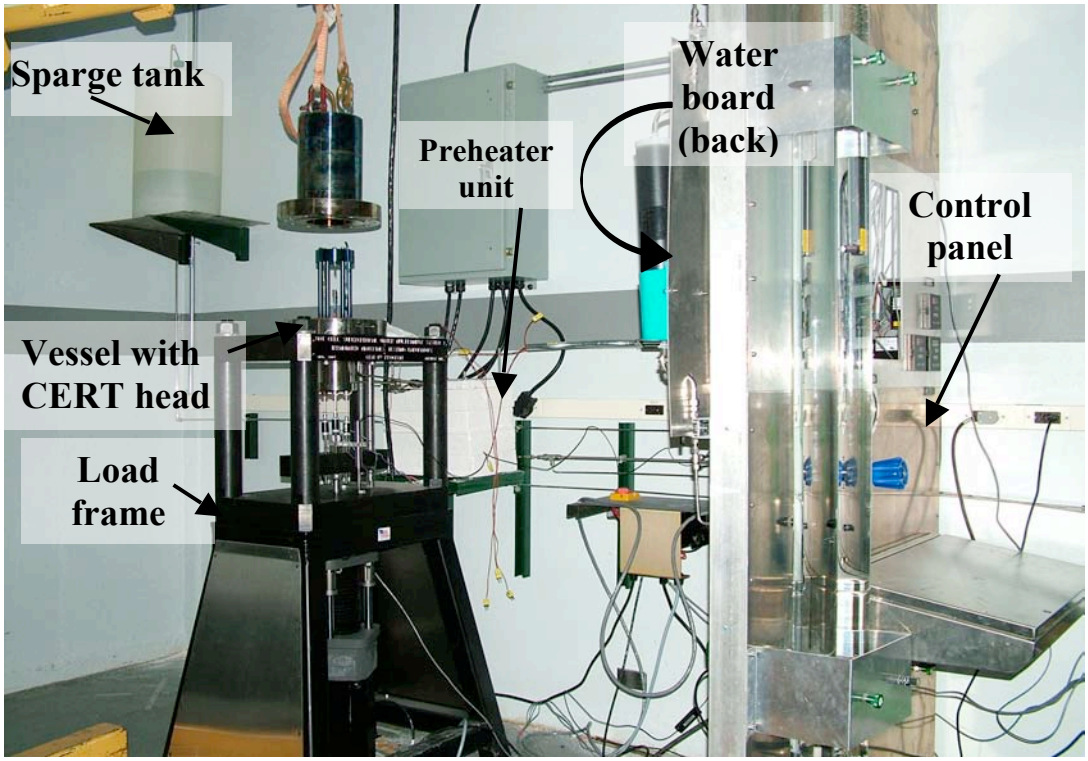

Figure 3. Photograph of the completed SCC test system for neutron-irradiated materials

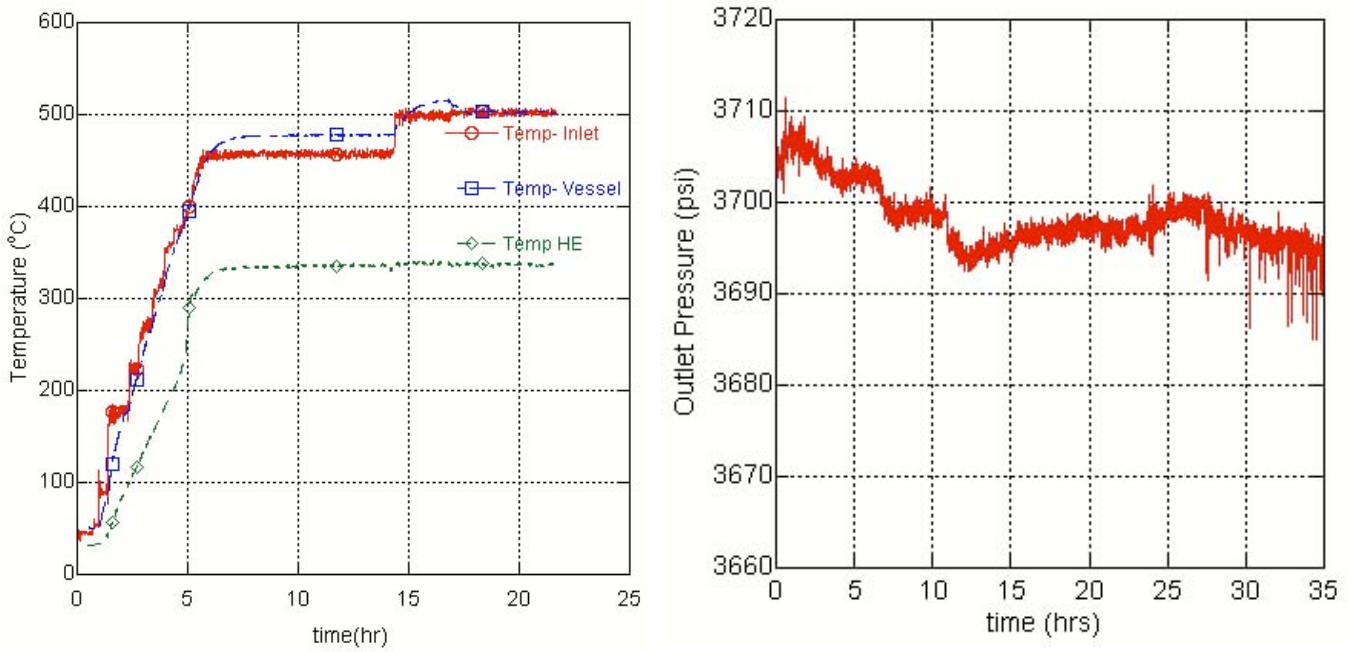

Figure 4. Temperature and pressure history for the demonstration test. The test was completed at the 22 hour mark.

2. Testing of the Operation of the Facility (dry-run)

The final step in qualifying the facility is the dry-run in which sample loading, vessel closure and test initiation are all conducted while treating the samples as if they were highly irradiated. Samples were successfully loaded, the vessel was sealed in the hot cell and pressure tested. The vessel and load frame assembly were then moved into IMTL and a 500°C deaerated SCW test was successfully initiated to complete the dry-run. The steps followed for the dry run were as follows:

1. Placement of the load frame - autoclave assembly in the hot cell and cell closure and installation of the guide board (that assists with sample assembly).
2. Opening of the lead pig and removal of samples.
3. Mounting samples into the clevises in a loading jig and mounting of the sample-clevis assembly into the autoclave.
4. Closure of the vessel.
5. Sealing of the vessel with the bolt tensioning system.
6. Pressurization test in the hot cell to ensure that it is free of leaks.
7. Removal of the bolt tensioning system.
8. Removal of the guide board.
9. Installation of heaters and insulation.
10. Transport of the load frame – autoclave assembly to IMTL.
11. Connection of the autoclave to the water supply, heating and pressurization system in IMTL.
12. Heat up and circulation of SCW for a tensile test.

These steps are described in detail in the following subsections.

2.1 Sample alloy and design

Samples with the same design as the first batch of neutron-irradiated samples identified for testing in FY2006 were used for the dry-run. The samples are “sheet samples” of the “W” design with a gage section of 0.094” wide by 0.02” thick. A total of four samples were used, each from a different alloy; 316L stainless steel, and nickel-base alloys 690, 625 and 718. Using 316L, 690 will permit to comparison of the data with that collected using the square cross-section samples in our laboratory. However, the yield strengths of 316L and 690 do not permit their use in the unirradiated state in supercritical water as the sample would yield due to the internal pressure. Therefore, we, we decided to use slightly thicker samples for 316L and 690. The schematic of the samples is presented in Fig. 5.

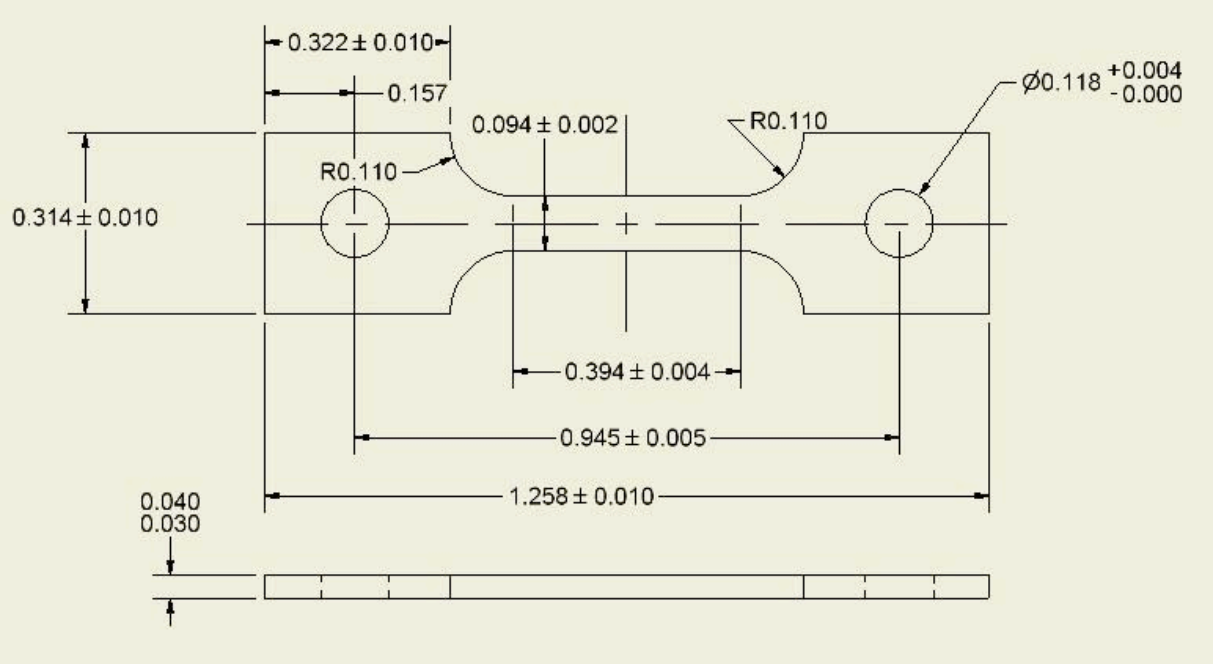

Figure 5. Schematic of the "W" sample design used for the dry-run.

2.2 Starting configuration

The hotcell was prepared as if radioactive samples were to be loaded. The vessel body is removed and installed on a stand, a guide board is installed with cameras attached, the guide rods for the autoclave body are removed, the flange tensioning system, heater bands and insulator are placed near the load frame, the clevises are stored in a box on the work space and the samples are in the lead pig in individual vials. Figures 6 and 7 show the hotcell at the starting state.

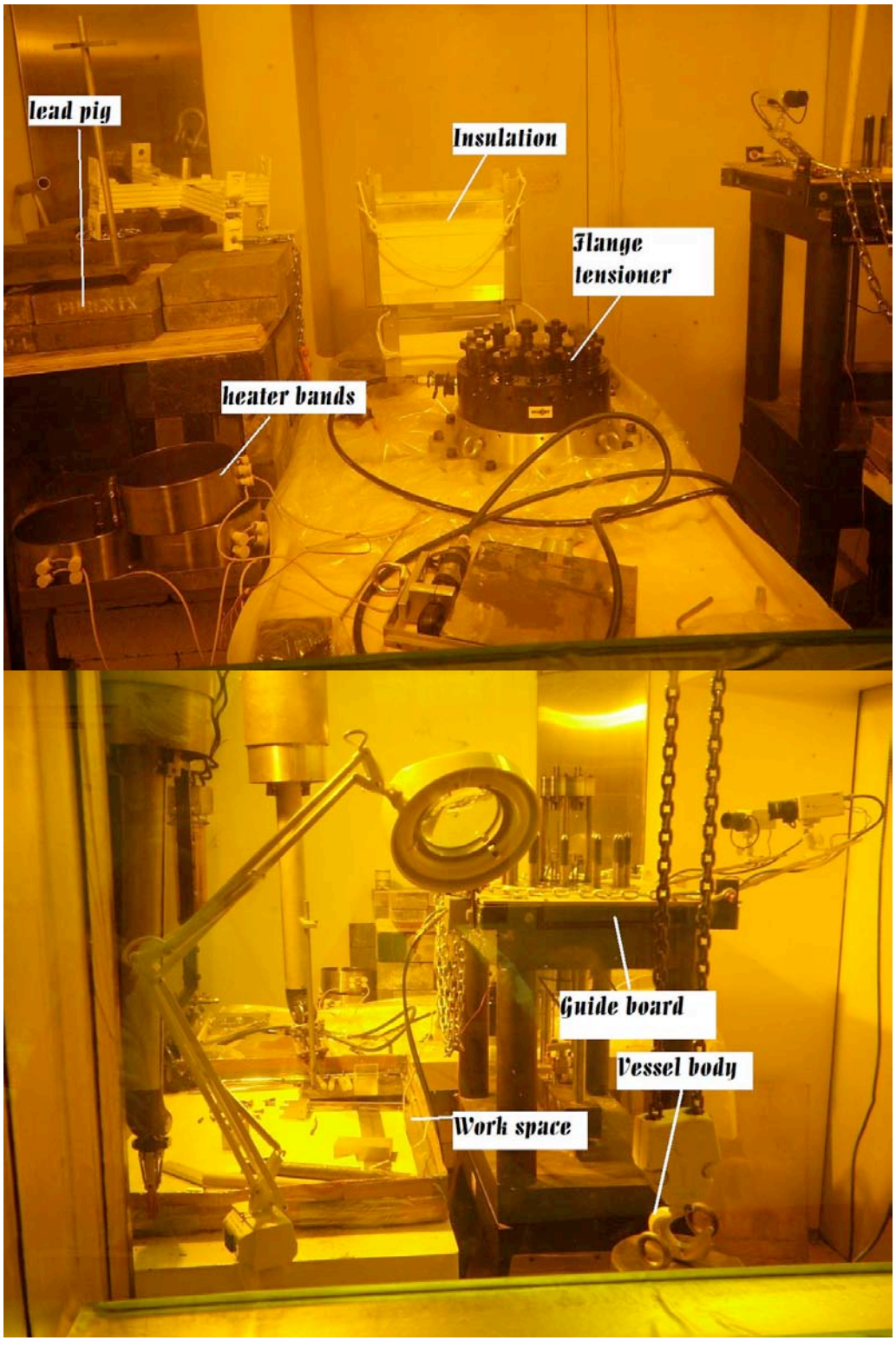

Figures 6 and 7: Overall view of the hot cell before the test. The room is set up as if samples were just removed from a previous test.

2.3 Removing the samples from the lead pig and installation in the clevis

Each vial is successively removed from the lead pig and the sample is removed from the vial. Figure 8 shows the vial containing the 316L sample being picked up by the manipulator. Each sample is then installed in its clevises.

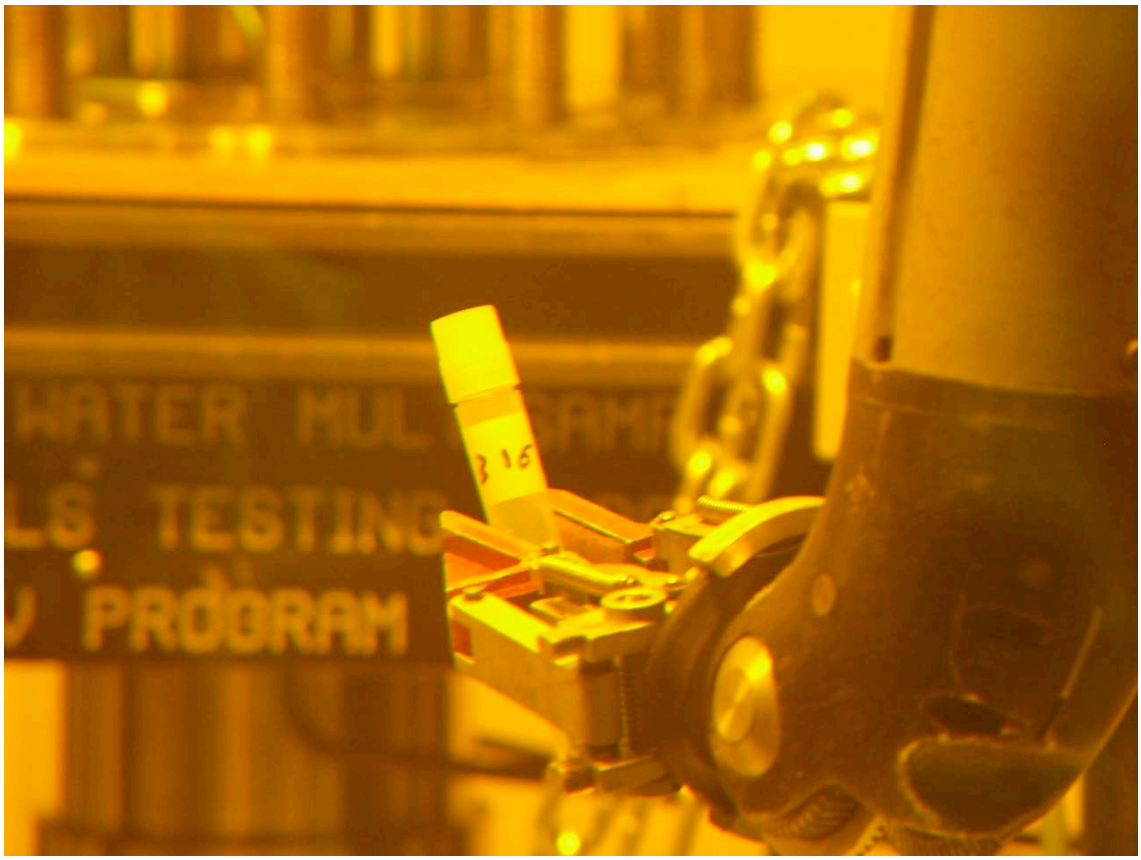

Figure 8. The vial containing the sample made of 316L being removed from the lead pig.

The samples are mounted in their clevises and thin wires were secured to the pins to prevent them from reaching the floor in case they are dropped. Considering the small size of the specimens, this operation is done using a specially made mounting jig and illuminated magnifier made for those clevises. Figure 9 shows the workspace used for this operation (this photo was taken after the samples were mounted).

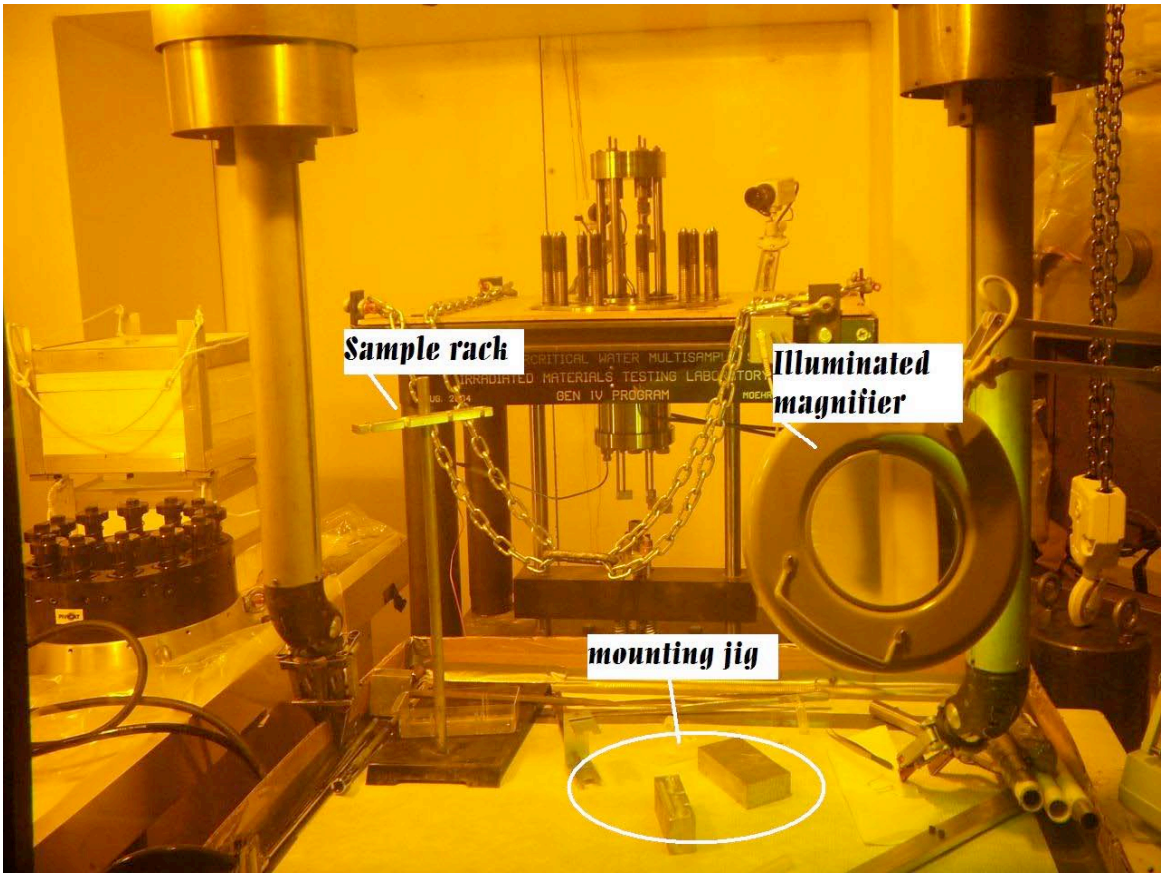

Figure 9. View of the workspace used to mount the samples in the clevis. The illuminated magnifier, the sample rack and mounting jig are visible.

2.4 Mounting the samples in the vessel

Once a sample had been inserted in the clevis, it is loaded into the loading jig as shown on Fig. 10. The cameras installed on the guide board assist the operator in mounting the samples at the back of the vessel as shown Fig. 11. Figure 12 shows the vessel with all four samples installed.

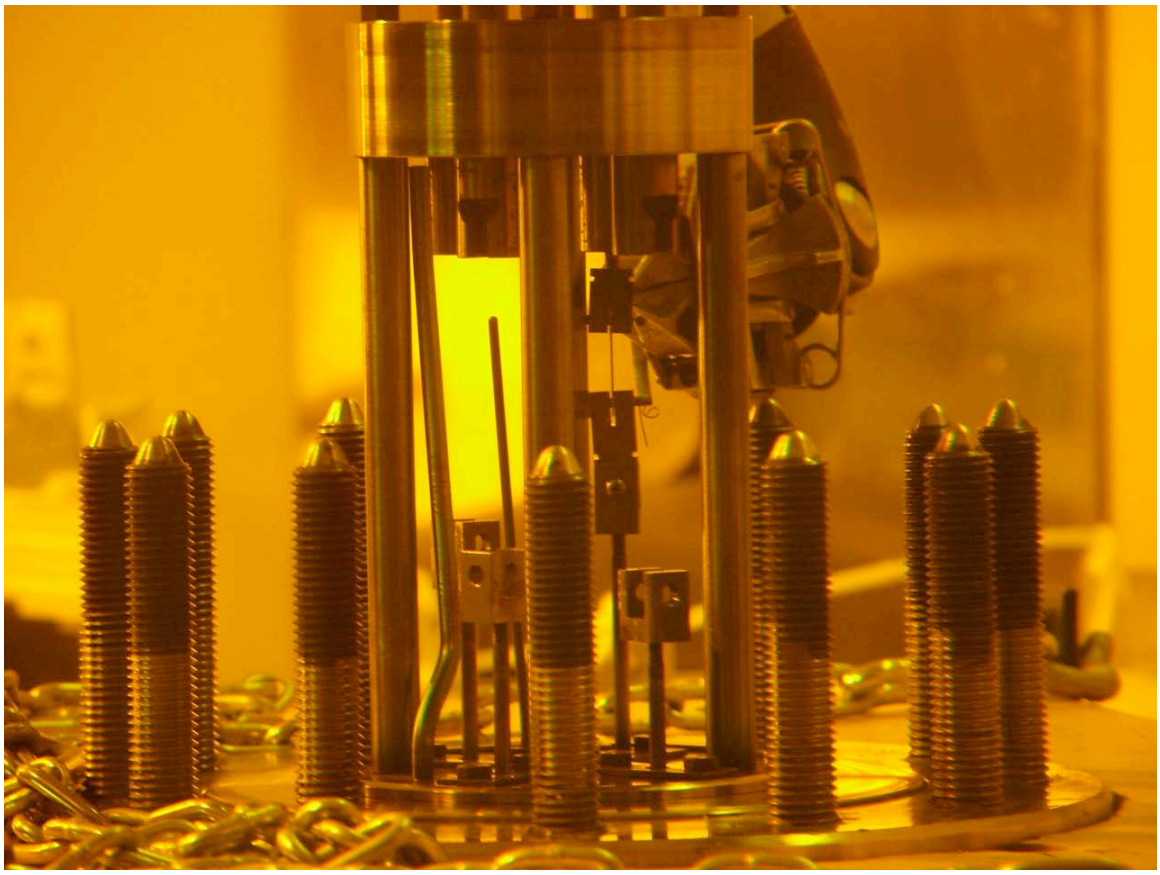

Figure 10. Loading of the first sample at the back of the vessel.

Figure 11. Installation of a sample with the assistance of the cameras located on the guide boards

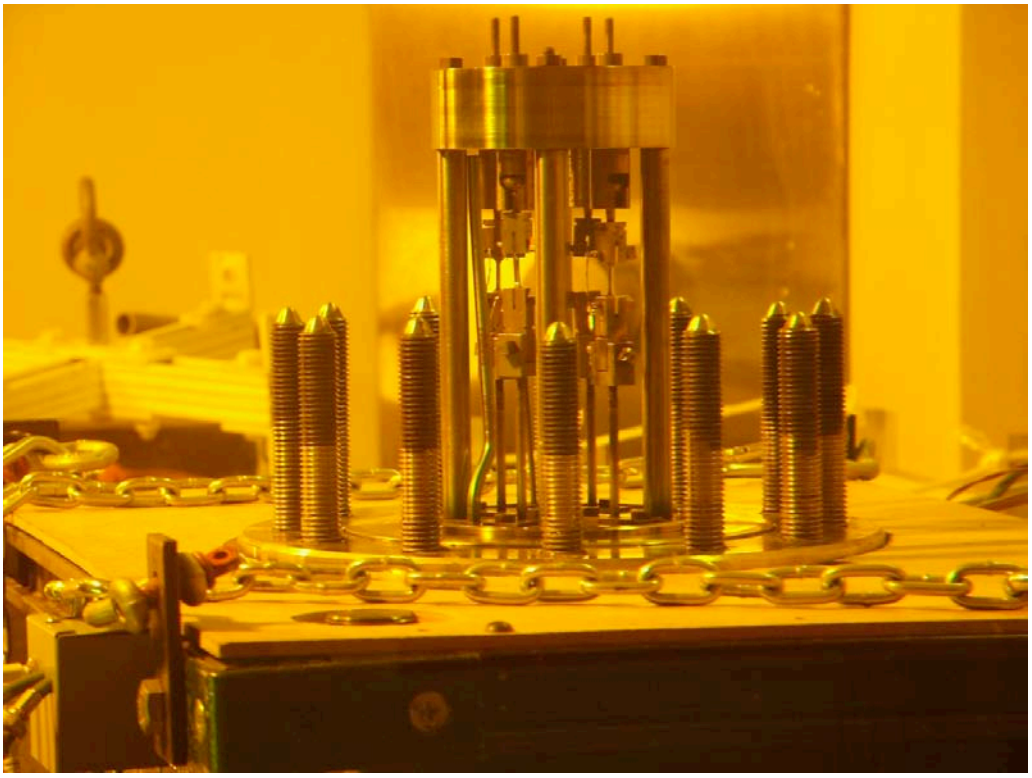

Figure 12. View of the vessel after the four samples had been mounted.

2.5 Closure of the vessel

Once the samples are installed, the guide rods are inserted into the guide board, the hoist picks up the vessel body and lowers it down over the head. This operation is illustrated in Fig.13. This operation is particularly delicate as the clearance between the sealing surface and the internal load frame is less than 0.25" and any scratch on the sealing surface could jeopardize the ability to the vessel to seal. After completion of this step, the vessel stands as shown in Fig. 14, with twelve studs protruding out of the flange, waiting for the nuts to be installed by the tensioner.

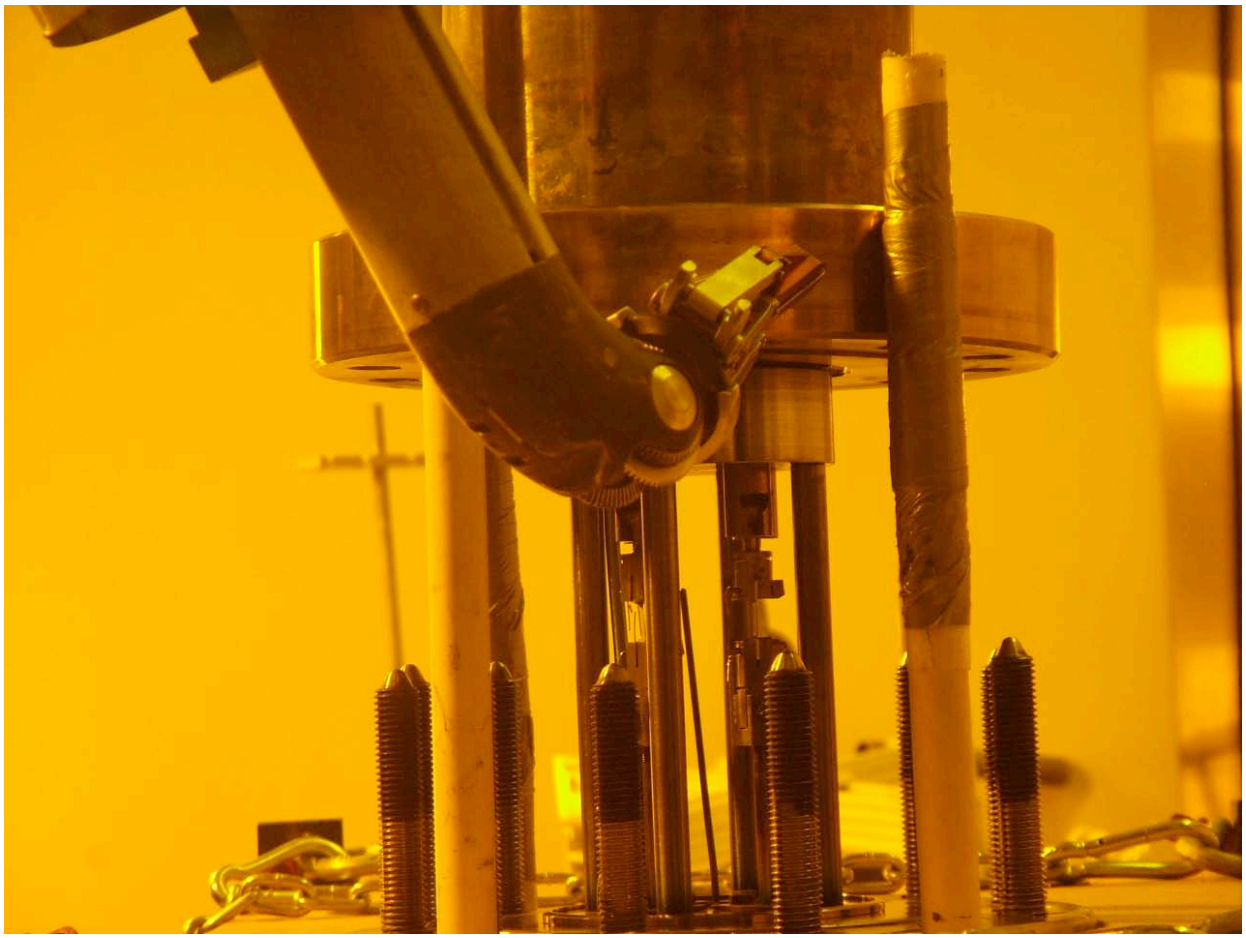

Figure 13. The vessel body is lowered down over the head once the samples have been installed.

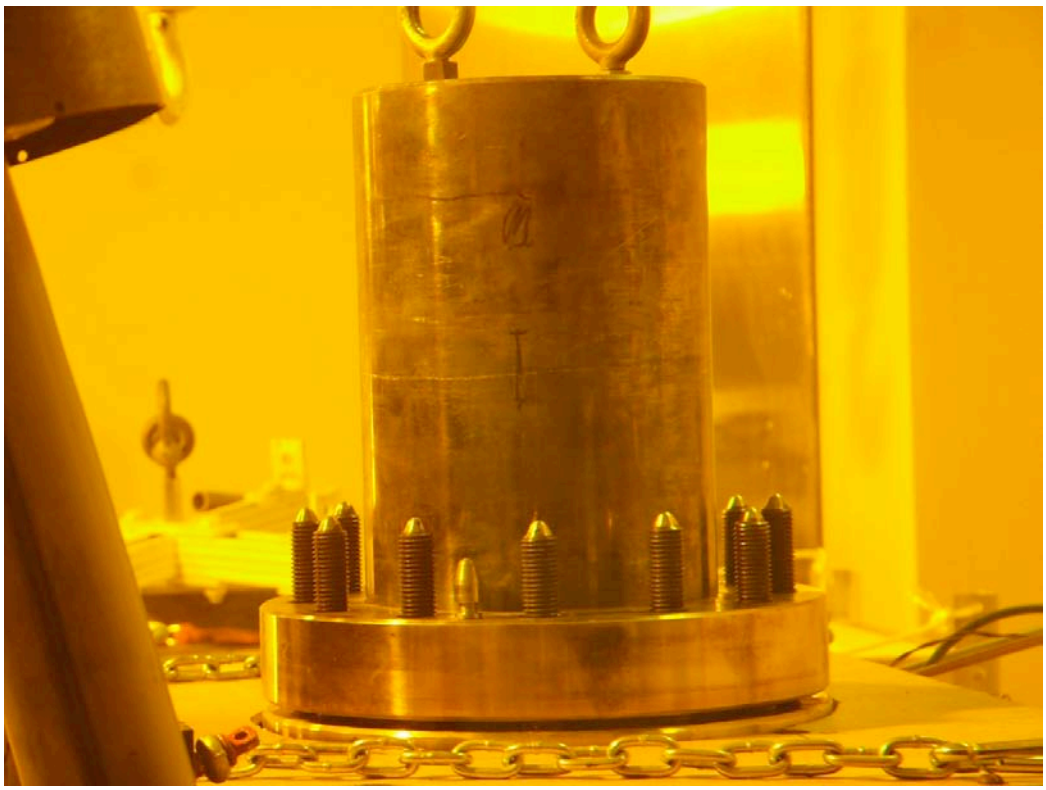

Figure 14. The vessel is closed and ready to be sealed.

2.6 Flange tensioner installation and sealing of the vessel

Once the vessel is closed, the hoist picks up the flange tensioner and installs it over the vessel body, Fig. 15. The manipulation of the 24 bolts and nuts prepare the flange tensioner for the sealing step, Fig. 16. Once the tensioner is in place, a hydraulic pump is activated to pull the studs and uniformly compress the sealing gasket. The operator actuates the flange tensioner to secure the vessel in this position, then the pressure is relieved and the vessel is sealed.

2.7 Pressurization test

The vessel is connected to a high-pressure pump and is filled with pure water and pressurized. Once the vessel was able to maintain pressure without leakage, the pressure is relieved and the tensioner can be removed.

2.8 Removal of the bolt tensioner

As the pressurization test proved that the vessel was sealed, the tensioner is removed. Figure 17 shows the tensioner being removed.

2.9 Removing the board

The guideboard and cameras are disconnected and removed, Fig. 18.

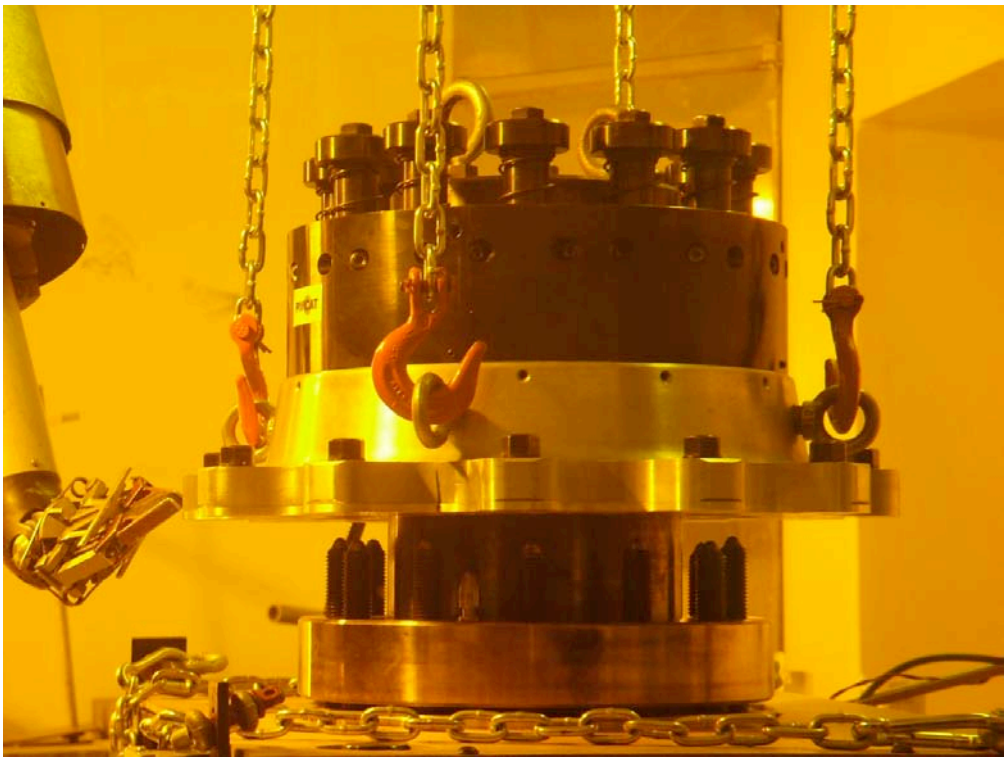

Figure 15. The flange tensioner is lowered down over the vessel.

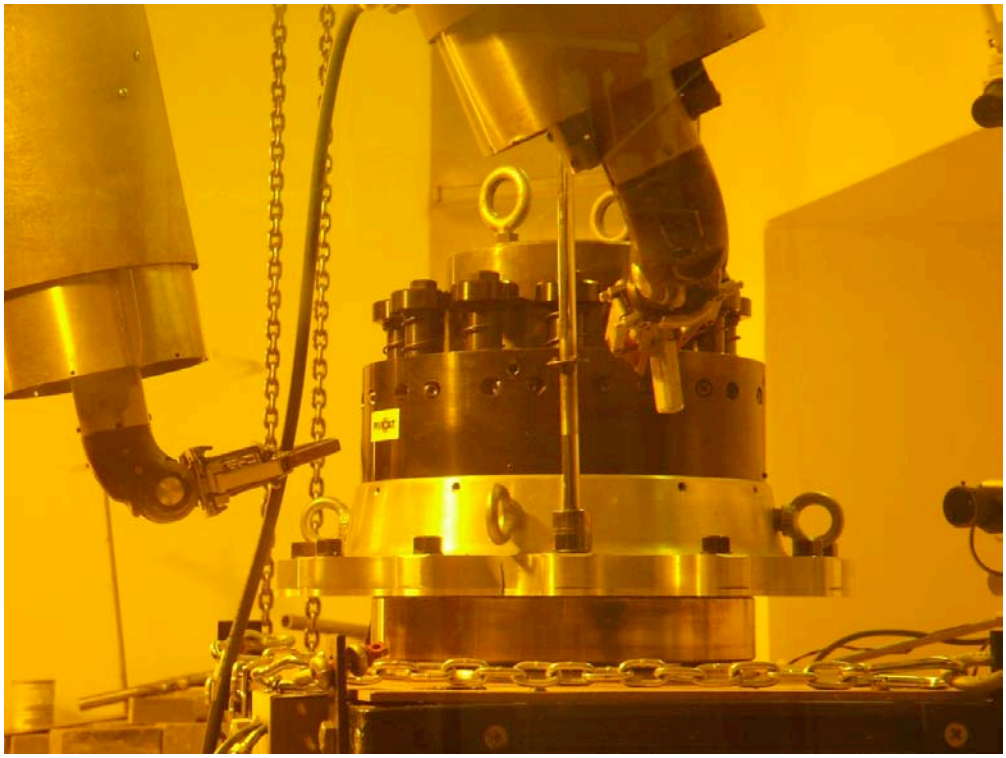

Figure 16. First step of the manipulation of the bolt tensionner: using a low power pneumatic wrench, the operator installs the nuts over the studs

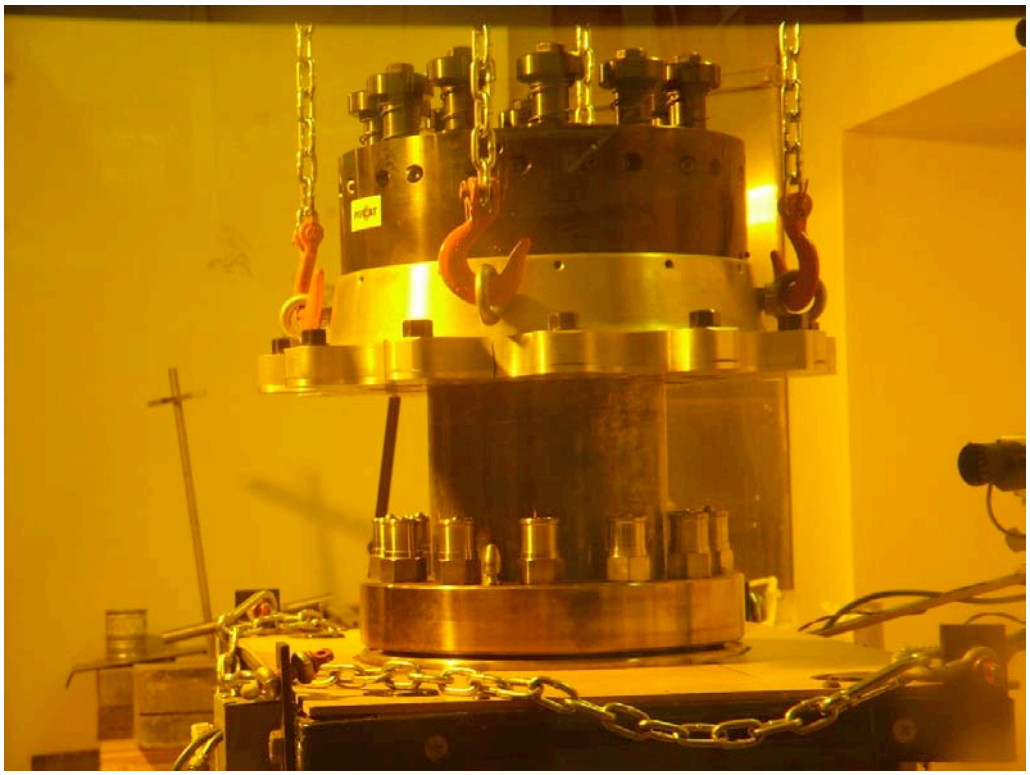

Figure 17.The flange tensioner is removed after installing the nuts over the studs and sealing the vessel.

Figure 18. Disconnection of the cameras before the guide board is removed.

2.10 Installation of the heaters and insulation

The heater bands are slid over the vessel body and tightened, Fig. 19. Then the insulation in installed over the assembly, Fig. 20.

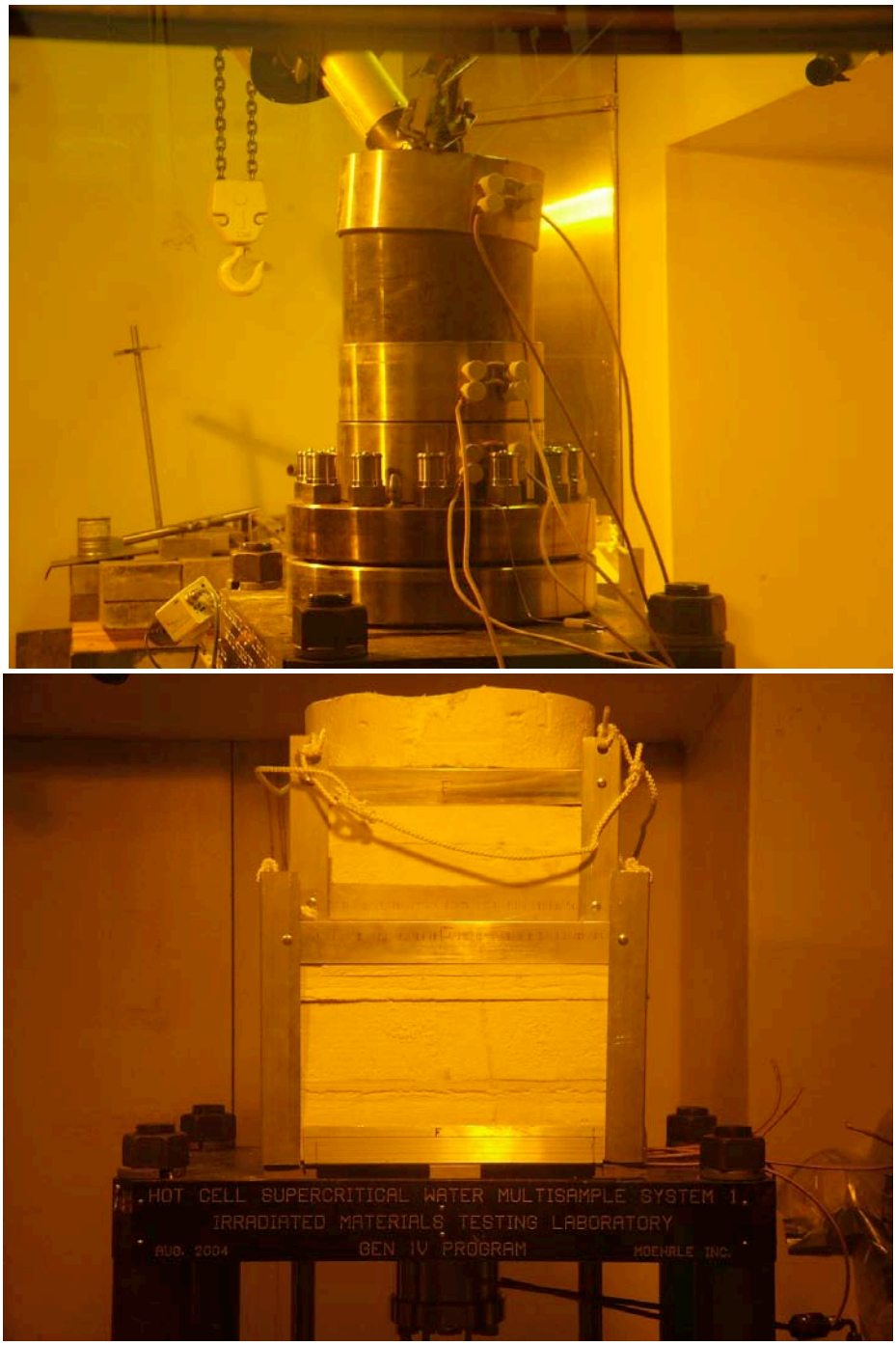

Figures 19 and 20. The heaters bands are clamped on the vessel body and the insulation applied over the bands.

2.11 Rolling the vessel out of the hotcell

If the samples were radioactive, an additional step would have been to install a shield around the insulation. This is a simple operation, but wasn't necessary in the present case and it will not be needed for the irradiated samples that will be tested in FY2006. Hence, the load frame was ready to be rolled outside the hotcell and into IMTL for connection to the water system as shown in Fig. 21.

Figure 21. The loading unit is ready to be rolled back into IMTL to begin the experiment.

3. Benchmark Experiments

3.1 CERT Test Mode

The benchmark test was conducted for comparison with existing data from a similar SCW system in our cold-laboratory. Four samples were strained to failure. They were 304LSS, 316LSS, 690 and 625 in 500°C SCW to match the results from our cold-lab facility. Straining was started after conditioning the system at 500°C for about 139 hrs when the water chemistry was stable at target conditions. Before starting the test, it was verified that all parameters were at or very near the target values with acceptable oscillations. The target condition of this experiments are summarized in Table 2. Stress-strain curves obtained during the test are compared to those obtained in the cold-laboratory in Fig. 22. As can be seen, the overall shapes of the curves and the relative behavior of the alloys between the two tests are similar. Alloy 625

is the strongest one among the four alloys and alloy 690 is the second strongest in both tests. The yield point, maximum stress and rupture strain of 316L and alloy 690 are very similar in both tests. The stress-strain curves of 304L samples between the two tests are close as well before the strain reaches 25%, at which point straining on the 304L sample during the reference test was stopped. Alloy 625 exhibits very high maximum stress and strain in the benchmark test. This can be attributed to the fact that the fracture location on alloy 625 sample was not in the gage section, but at the end of the threaded section. This unexpected fracture location implies that defects resulting in high stress concentration were produced when machining the threads on the sample, which is not related to the performance of the test facility.

Analysis of the test results also includes estimation of crack density, crack length, crack length per unit area, crack depth and crack growth rate, and characterization of cracking modes based on observations of the gage surfaces, fracture surfaces and cross-sections. The results of the analysis are given in Table 3, in which the corresponding results of the reference test are also listed for comparison. The comparison shows good agreement in terms of the trends of the changes of cracking behavior of alloys. Furthermore, the crack length per unit area and crack growth rate (CGR) for 316L and Inconel 690 are very similar in both tests. The cracking behavior of 304L and Inconel 625 in the two tests shows relatively large differences. This can be attributed to the fact that the experiment on 304L was stopped at 25% elongation in the reference test, and that the fracture surface of Inconel 625 in the benchmark test is not in the gage section.

Typical SEM photos of the gage surfaces and cross-sections are shown in Fig. 23. Analyses of both the cross-section and gage surface observations indicated that most cracks on the gage section of 304L and Inconel 625 were intergranular. The same was true for 316L and 690 except that there was also transgranular cracking on the gage surface. These analysis results are similar to those of the reference test.

In general, precise analysis of the benchmark test results showed good agreement with the reference test, which further confirmed the validity of the operational capabilities of the hot SCW test facility for conducting CERT experiments.

Table 2. Conditions used for the benchmark test

Pressure (MPa)	25.5
Temperature (^{o}C)	500
Conductivity (μS/cm)	<0.1
Dissolved oxygen (ppb)	<10
Tensile samples	• 304L • 316L • Inconel 625 • Inconel 690
Strain rate	$3 \times 10^{-7} s^{-1}$

Table 3. Summary of stress-strain and cracking results for benchmark and reference tests

Tests	Alloys	Yield strength (MPa)	Maximum strength (MPa)	Rupture strain (%)	Fracture mode	Crack density (#/mm^2)	Crack length (μm)	Crack depth (μm)
Benchmark	304L	185	420	36.8	IG+ductile	59.3	46.8	49.9
	316L	190	370	36.6	ductile	23.3	46.8	23.0
	625$^+$	335	960$^+$	60.7$^+$	IG+ductile	504.9	15.5	13.6
	690	215	475	41	IG+ductile	19.8	32.6	27.7
Reference	304L*	120	340*	25*	Did not fail	39.4	32.2	51.4
	316L	140	350	33	ductile	38.1	28.5	24.9
	625	270	675	47	IG+ductile	137.1	42.4	84.2
	690	174	455	42	Granular +ductile	32	24.9	33.1

+ Fracture surface is not in the gage section.

* Experiment stopped at 25% elongation. The maximum stress and ultimate strain may be anomalistic.

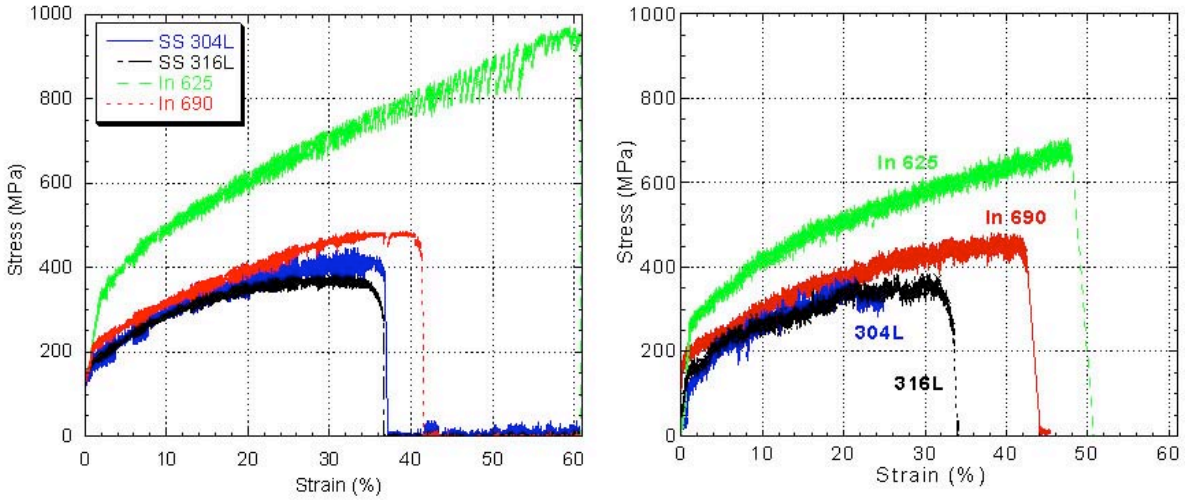

(a) (b)

Figure 22. Stress-strain curves from the benchmark test. (a) Test results from IMTL and (b) test results from cold-lab (HTCL).

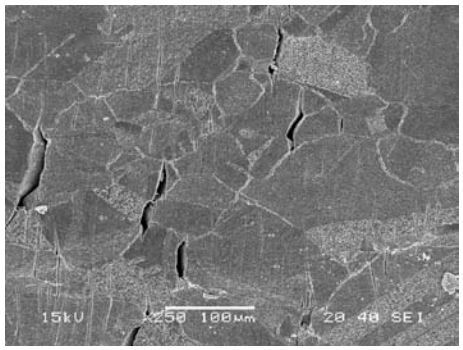

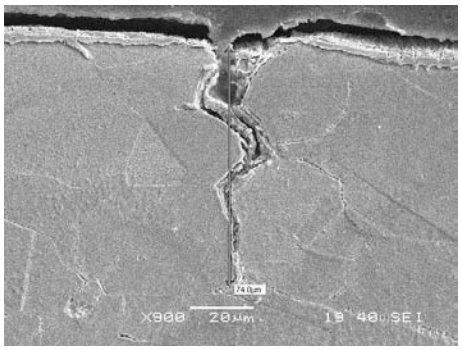

304L

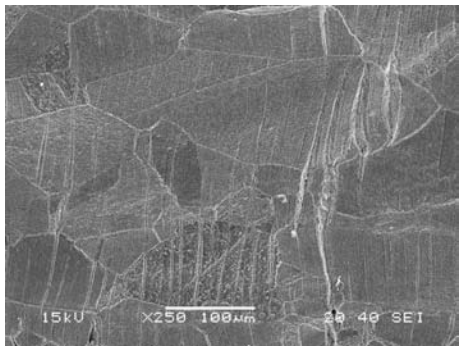

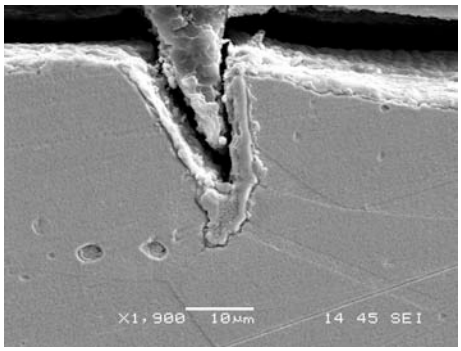

316L

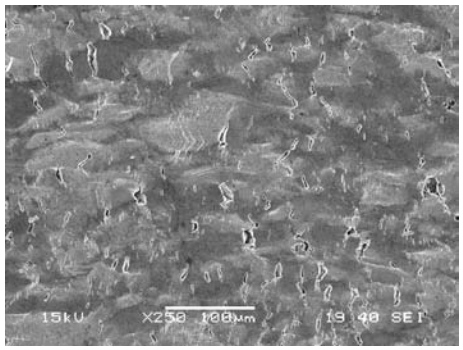

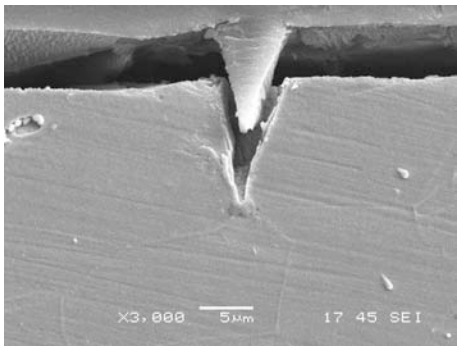

625

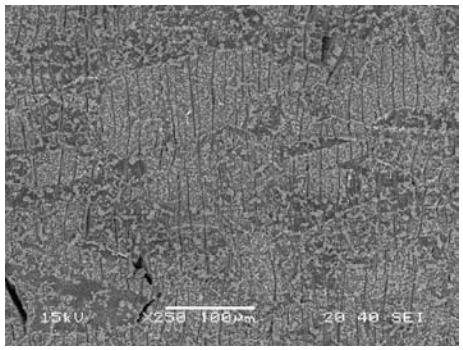

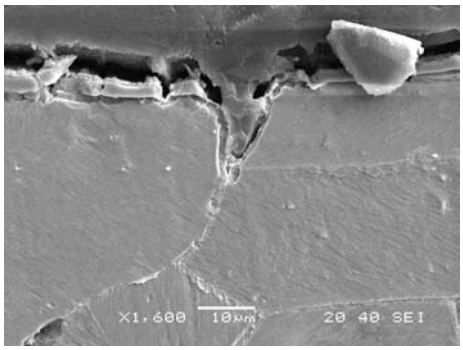

690

Figure. 23. EM observations of gage surfaces and cross-sections of 304L, 316L, Inconel 625 and Inconel 690.

3.2 CGR Mode

The autoclave and load frame system was used in CERT mode for system demonstration, benchmarking and a dry-run because of existing institutional experience in CERT and a database for CERT tests in SCW. Benchmark activities related to crack growth rate (CGR) mode focused on a fatigue CGR test to validate the methodology and instrumentation for CGR determination. This section describes CGR measurement instrumentation and the results of that benchmark experiment.

3.2.1 The Direct Current Potential Drop System for Measuring Crack Extension

The components specially required for conducting CGR experiments include the direct current potential drop (DCPD) system, an autoclave head dedicated for CGR testing, the internal load frame, load linkage and clevises, the Conax fitting through which the current and potential probes of the DCPD system pass to the outside of the autoclave, and a motor capable of applying high frequency (≥1HZ) cyclic loading. The DCPD system for measuring crack extension plays a key role in CGR experiments. Fig.24 shows a schematic drawing of the system. The CT sample is instrumented with Pt current and potential probe leads, which are necessary to insure secure, lasting connections to the sample. The DC source supplies high stability current to the CT sample, which is reversed periodically through the solid state relays in order to correct for thermocouple effects. The potential drop resulting from crack extension in the sample is measured by the nanovolt meter. A dedicated software program run on the PC controls the nanovolt meter, the DC source and the relays through IEEE-488 interfaces and a parallel port, for the purpose of achieving data acquisition, current reversal, crack extension calculation and load control for constant stress intensity factor (K) CGR experiments. The PC also supplies 0 to 5 volt signals needed to control the relays. The measurement process can be described as follows:

1. Reverse the direction of the current flowing through the sample.
2. Take a measurement of the probe potential.
3. Repeat steps 1 and 2 and average the absolute values of the two potential readings.
4. Continue the sequence 30 to 2000 (or more) times, and average the readings (N_{avg}) to form a single data point. Increasing N_{avg} improves the measurement resolution.

The Pt current and potential probe leads are connected to the CT sample by spot welding. Since the locations of the probes on the sample faces affect the accuracy of the DCPD measurement, spot-welding is a critical step in the process. In general, the current probes are placed in the center of the width of the top and bottom faces of the sample, and about 5 mm from the back. The potential probes are placed on opposite corners of the machined notch, on the sides of the sample within about 1mm of the corner, Fig. 25. The pictures shown in Figure 26 (a) and (b) give an example of the CT sample that is mounted on clevises along with the spot-welded probe leads on it.

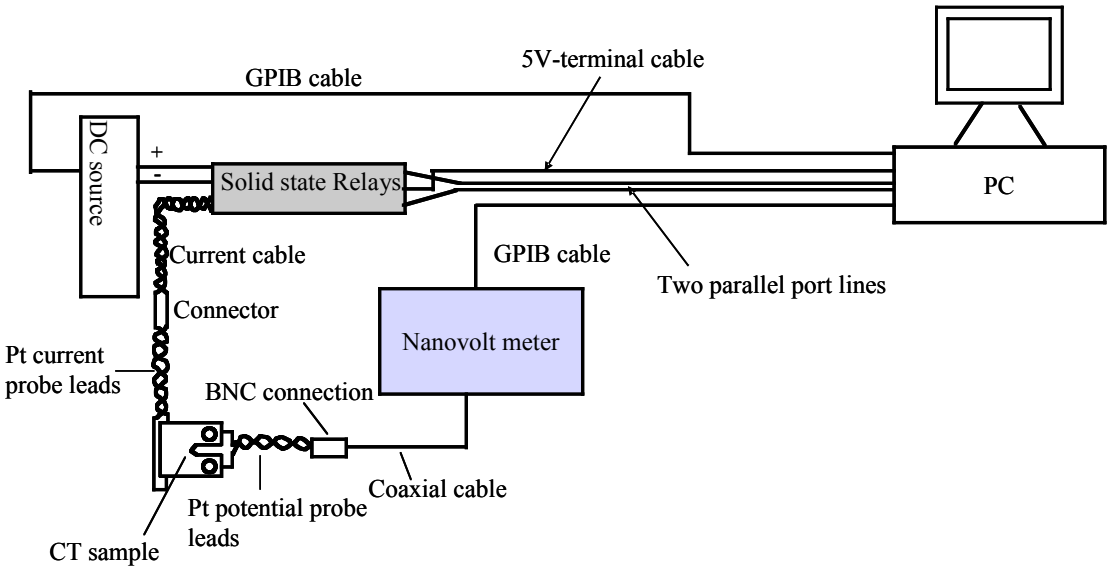

Figure 24. A schematic drawing showing the configuration of the DCPD system.

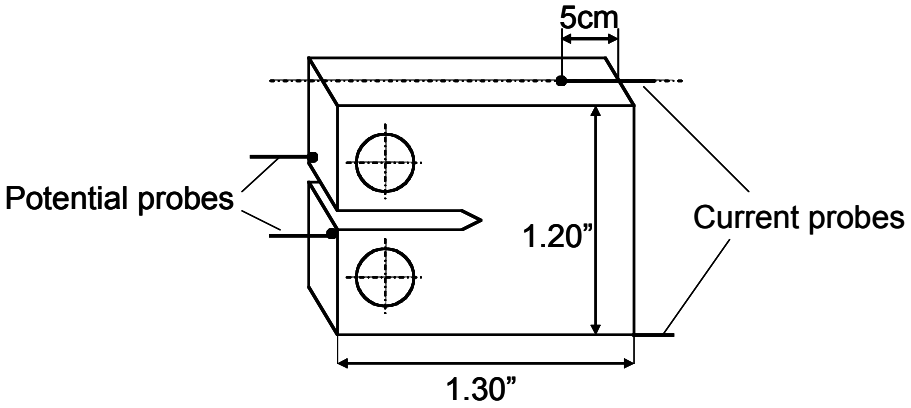

Figure 25. A schematic diagram showing the placement of the probes on the CT sample

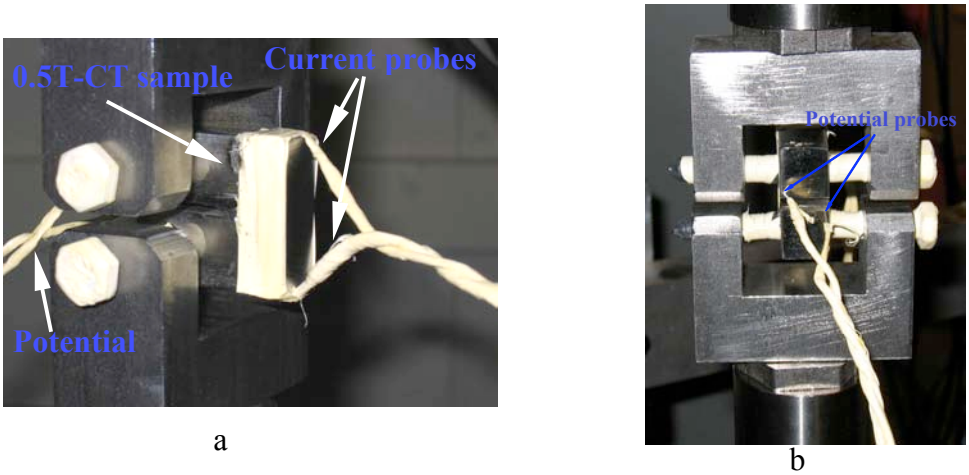

a b

Figure 26. (a) and (b). Pictures showing a CT sample mounted on the clevises and the current and potential probe leads spot welded on the CT sample.

3.2.2 Resolution and Accuracy of DCPD Measurement in a Fatigue CGR Test

In order to establish the resolution and accuracy of the DCPD system for measuring crack extension in CT samples, a six-step fatigue crack growth rate test of a stainless steel 0.5T-CT sample under varying R (ratio of minimum load to maximum load) conditions was performed, Table 4. The purpose of the changes in R ratio was to produce beach marks on the fracture surface that allow for measurement of the crack length on the fracture surface of the sample (post-test) and for benchmarking the DCPD measurements. Six steps were employed for the test to provide sufficient crack growth rate data for benchmarking the DCPD measurements.

As described previously, current and potential leads were spot-welded on faces of the CT sample with required locations for DCPD measurements. Then the sample was mounted on clevises to be cyclic loaded by an MTS machine. After the test was initiated, the frequency was reduced in order to drop the rate of crack growth. Also during the test, the N_{avg} was increased from 300 to 1200-1500 to improve the measurement resolution.

Table 4. Loading conditions for each step in the fatigue test

Steps	Loading Conditions
Step 1	Sine Waveform, F=0.2-1HZ, R=**0.1**, initial K_{max}=15MPa $m^{0.5}$, Lmax=3.776kN. Constant maximum and minimum load, crack length increment: 538μm. a/w=0.4347-0.4558.
Step 2	Sine Waveform, F=0.06-0.5HZ, R=**0.5**, Lmax=3.776kN, constant maximum and minimum load, crack length increment: 445μm. a/w=0.4558-0.4732.
Step 3	Sine Waveform, F=0.04-0.5HZ, R=**0.1**, Lmax=3.776kN, constant maximum and minimum load, crack length increment: 517μm. a/w=0.4732-0.4935.
Step 4	Sine Waveform, F=0.04-0.5HZ, R=**0.5**, Lmax=3.776kN, constant maximum and minimum load, crack length increment: 500μm. a/w=0.4935-0.5131.
Step 5	Sine Waveform, F=0.02-0.5HZ, R=**0.1**, Lmax=3.776kN, constant maximum and minimum load, crack length increment: 500μm. a/w=0.5131-0.5327.
Step 6	Sine Waveform, F=0.02-0.5HZ, R=**0.5**, Lmax=3.776kN, constant maximum and minimum load, crack length increment: 500μm. a/w=0.5327-0.5523.

Note for abbreviations: K, stress intensity factor, F, the frequency of the cyclic loading, L, load applied to the sample, a, the crack length and w, the width of the CT sample.

Following completion of the test, crack extension measured by DCPD was plotted as a function of time to determine the measurement resolution. The amount of crack extension produced during each step of the fatigue test was measured using an optical microscope in order to compare against crack extension determined from the DCPD measurement. Errors in K due to errors in the DCPD measurement were evaluated as well.

The fracture surface of the CT sample clearly shows the crack extension produced in each step of the six-step fatigue test under varying R, Fig. 27. These crack extensions are compared with the DCPD measurement to determine a cumulative crack extension as a function of steps of the fatigue test, Fig. 28. The difference between the two measurements before step 4 is very small. From steps 4 to 6, the difference gradually increased to a final value of 0.18 mm.

Resolution of the DCPD measurement is strongly affected by N_{avg} and crack growth rate. Increasing N_{avg} to 1500 readings and decreasing the crack growth rate by reducing the frequency of the fatigue loading improved the measurement resolution to about 3-5μm, Fig. 29. This resolution is sufficient for normal crack growth rate tests with a minimum crack extension of hundreds of micrometers.

One of the main concerns of constant K, CGR experiments is the error in K due to the error in the estimated crack length. This error is shown in Fig. 28 for the benchmark test. The error in K was calculated based upon an assumption that a crack was growing in a side-grooved 0.5T-CT sample under a typical constant K of 20MPa $m^{1/2}$. The maximum error in K due to the maximum error in the DCPD measurement (0.18 mm) is 0.45MPa $m^{0.5}$. This is very small compared to the target values of 20 MPa $m^{1/2}$ and will not result in a significant difference in the measured crack growth rate.

In general, the completion of components for CGR measurement and the resolution and accuracy of the DCPD measurement attained in the benchmark fatigue CGR test has established that the experimental facility is ready for crack growth rate testing in high temperature water. The first CGR test planned for FY2006 will be on 316L in 288°C BWR water, followed by a test in SCW over a range of temperatures.

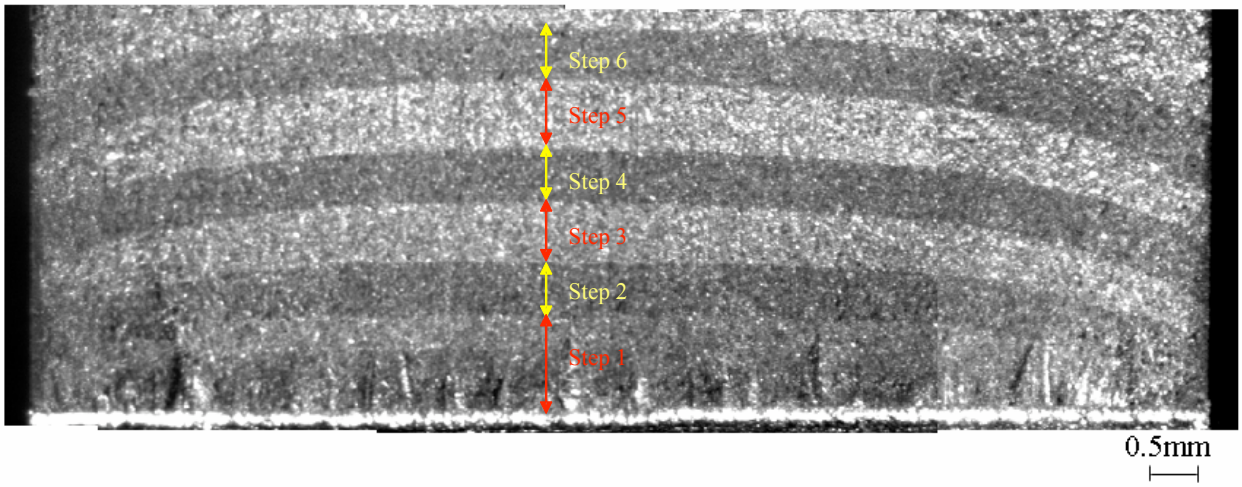

Figure 27. Fracture surface of the CT sample following the fatigue CGR test. Crack extensions produced during each step of the fatigue test under various R (0.1 and 0.5) are identified by the alternating light and dark bands. Crack propagation direction is from bottom to top.

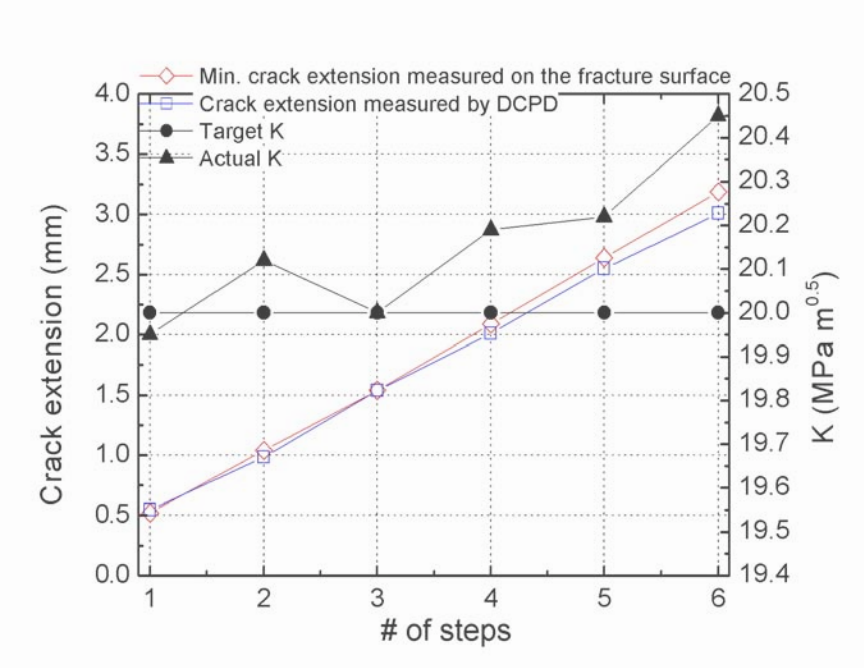

Figure 28. Comparison of crack extension measured by DCPD and post-test fracture analysis as a function of steps in the fatigue test. The figure also shows the difference between the target K and the actual K in an assumed constant K test that varies due to errors in DCPD measurement of the crack extension.

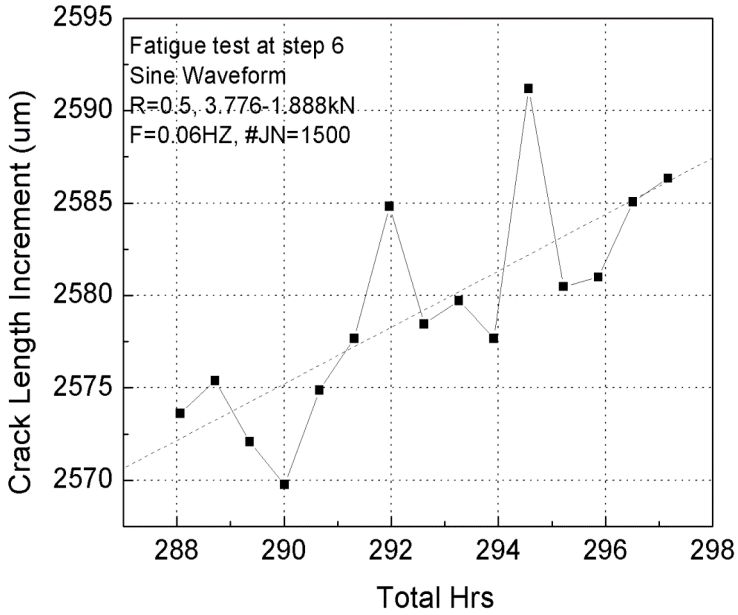

Figure 29. Crack length vs. time, showing the resolution of DCPD measurement attained at step 6 of the fatigue CGR test. In order to obtain high resolution, N_{avg} was increased to 1500 and the crack growth rate was lowered to about 1.5μm/hr by reducing the fatigue loading frequency to 0.06HZ.

4. SEM Installation

A Scanning Electron Microscope JEOL Model JSM-6480 was received and installed. The SEM is equipped with a Everhart Thornley detector for secondary electron imaging and a backscattered electron detector that provide compositional, topographic and shadow image. It also has a Genesis 2000 XMS System 60 Energy Dispersive Spectrometer from EDAX. The EDS has a sapphire detector with a 130 eV. resolution

The diffusion pump, usually installed in such microscope, was exchanged for a turbomolecular pump to eliminate the need for water recirculator and hence ease the installation of the microscope in a hotcell.

5. Operational Check out of the SEM

The SEM is to be used to observe the fractaure and gage surfaces of irradiated specimens in the hotcell. Hence, the microscope column must operate in the hotcell and communicate with the control console outside of the hotcell. The installation of the microscope in the hotcell is relatively straightforward. The only adjustment to be done is due to the fact that the microscope was equipped with a fan to draw air from the floor to the inside assembly for cooling. As the hotcell floor is a potential source of contamination, to the fan was reconnected to an external air source so as to assure that no contamination was drawn into the SEM.

Figures 30 and 31 show the microscope column installed in the hotcell with the control console outside. Installation of specimen in the microscope was performed with the manupulators. Figure 32 shows the installation of a sample with the column in the hotcell.

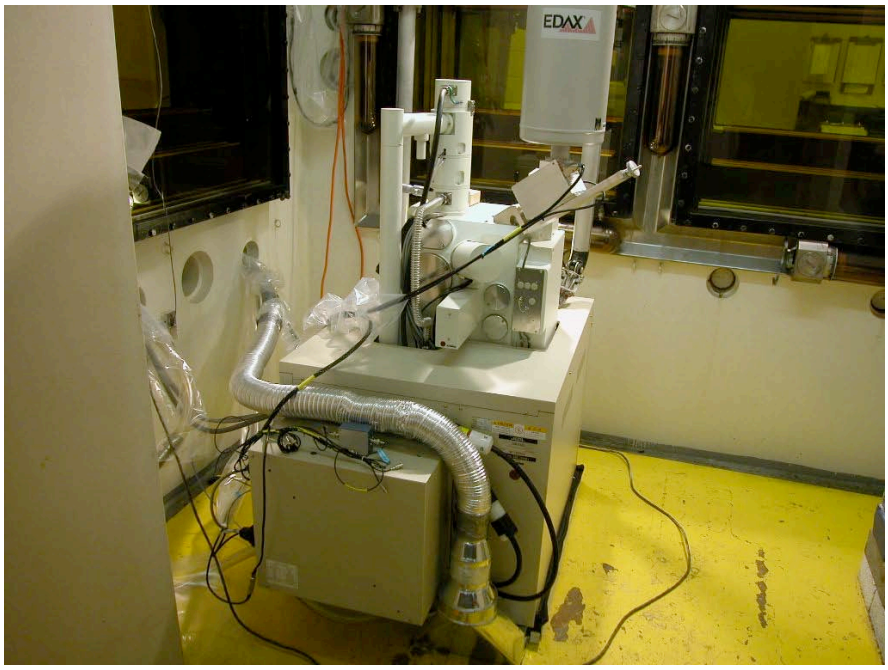

Figure 30. SEM installed for observation of irradiated specimen in the hotcell. Note that the microscope is installed on a “pan” that provides “clean” air to cool the microscope.

Figure 31. The microscope control located outside the hotcell.

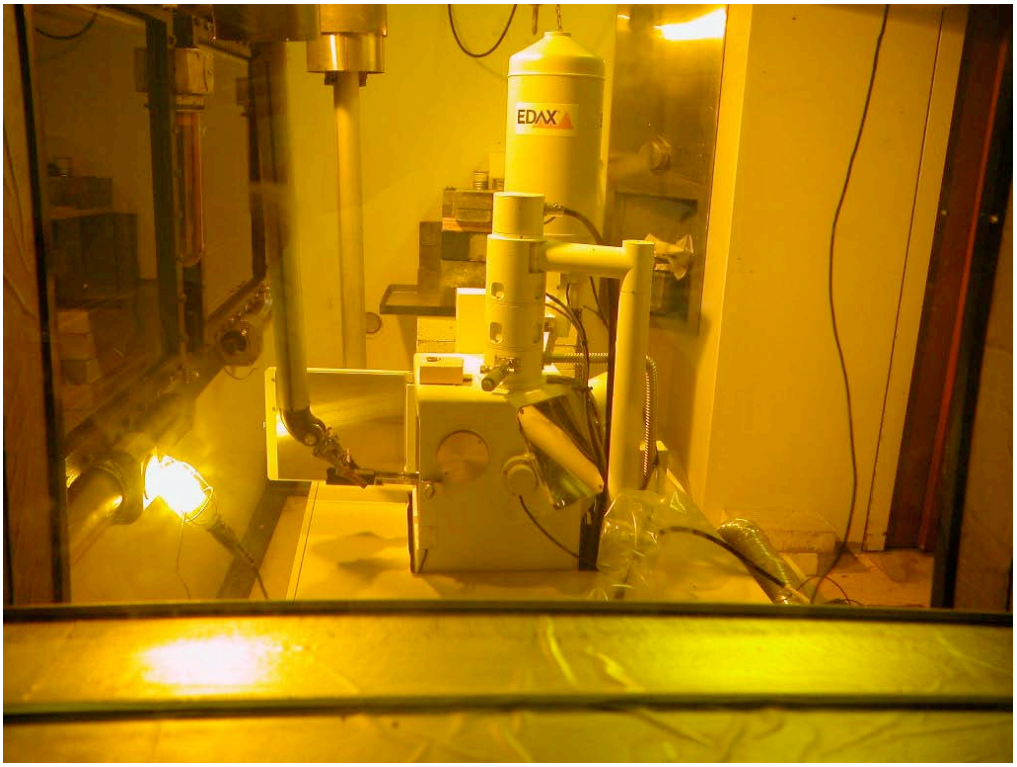

Figure 32. installation of a specimen in the SEM chamber in the hotcell.

6. License for Handling Radioactive Material

Based upon calculation of the activation in the FFTR samples, the current University Broad Scope license will allow for receipt of at least 100 JPCA samples from the Japanese fusion program irradiated at FFTF in the early 1990s. No amendment is needed to receive the quantities of radioactive materials in the estimated activity table below.

When the Supercritical water test program was contrived 36 months ago, the only known source of irradiated samples of potential reactor pressure vessel alloys to be tested in the UM corrosion loop were irradiated at a thermal reactor facility. Thermal reactor facilities such as the High Flux Isotope Reactor in Oak Ridge, the Ford Nuclear Reactor at the University of Michigan, and the Missouri University Research Reactor, typically have a fast neutron flux, which is a factor of 10 less than the thermal neutron flux. This high thermal neutron flux produces high quantities of thermal activation products (Co-60, Fe-55, etc) in the irradiated alloy targeted for a specific dpa. These higher quantities of radionuclides result in quantities of radioactive materials which can readily exceed limits on broad scope licensees such as that held by UM, impact on Emergency Planning requirements (10CFR30.32(1)) and financial assurance for decommissioning requirements (10CFR30.35).

Table 5. Estimated activity from W samples irradiated in FFTF.

	Max Specific Activity (micro Ci per gram)	Max Act per Sample (micro Ci)	Max Act Total (micro Ci)
C-14:	1.18E-05	1.18E-05	1.18E-03
Ca-45:	2.52E-02	2.52E-02	2.52E-00
Co-58:	1.33E-17	1.33E-17	1.33E-15
Co-60:	1.40E+02	1.40E+02	1.40E+04
Cr-51:	7.63E-52	7.63E-50	7.63E-50
Fe-55:	7.52E+02	7.52E+02	7.52E+04
Fe-59:	1.73E-32	1.73E-30	1.73E-30
Mn-54:	2.28E-01	2.28E-01	2.28E+01
Ni-59:	2.09E+01	2.09E+01	2.09E+03
Ni-63:	2.05E+03	2.05E+03	2.05E+05
P-33:	1.98E-62	1.98E-62	1.98E-60
S-35:	3.37E-19	3.37E-19	3.37E-17
Sc-46:	5.63E-18	5.63E-18	5.63E-16
Total	2.96E+03	2.96E+03	2.96E+05

NOTES: 1) FFTF Shutdown in 1992, 14 years of decay assumed.
2) 44 dpa assumed, equivalent to ~ 1 x 10^{23} n/cm^2 (fast flux)
3) Lethargy flux for energies between 0.1 and 1 MeV is 2 x 10^{14} n/cm^2
4) Lethargy flux for energies less than 0.001 MeV is 1 x 10^{13} n/cm^2
5) Alloy Japan PCA with composition taken as: Fe-14, Cr-16.2, Ni-2.3, Mo-0.24, Ti-0.4, Si-0.05, C-0.01, P-0.003S

UM has identified samples from the Fast Flux Test Facility (fast flux ~2 x 10^{14} n/cm^2 and thermal flux ~1 x 10^{13} n/cm^2) with a factor of 100 decrease in thermal activation products (e.g. Co-60, Fe-55, etc.) present in a sample of a given target dpa. The estimated activity for the samples of the highest dpa expected to be received from PNL is given in Table 5.

7. Identification of the First Batch of Neutron Irradiated Samples for Testing in FY2006

We are requesting a total of 21 tensile (W) samples of the JPCA alloy irradiated in MOTA for testing in supercritical water in order to determine the effect of irradiation on the SCC susceptibility of this alloy and also to provide baseline mechanical property data.

Through the U.S. SCWR program, stress corrosion cracking tests have revealed that austenitic alloys (both iron-base; 304L and 316L and nickel-base; 625 and 690) are susceptible to IGSCC in supercritical water at temperatures between 400 and 550°C. Irradiation of 304L, 316L and alloy 690 with 3 MeV protons to a dose of 7 dpa at 500°C and subsequent CERT testing in deaerated SCW at 500°C revealed a significant increase in the amount of cracking. While these experiments are continuing, the effect of irradiation on SCC in SCW needs to be verified with neutron-irradiated samples in order to definitively establish that neutron irradiation is detrimental to intergranular stress corrosion cracking in this alloy system in the conditions anticipated for the core of the SCWR.

The JPCA alloys are ideal candidates for this type of experiment as they have undergone significant irradiation to doses and temperatures that are relevant to the SCWR program. As part of our program, we propose to conduct a set of experiments in inert environment to establish baseline mechanical property behavior for these samples. Then we propose to conduct tests in supercritical water at or below the temperatures at which they were irradiated, to study the effect of the SCW environment on cracking propensity. Depending on the outcome of the tests in deaerated SCW, a second set of tests is planned in SCW containing either dissolved oxygen (more aggressive) or dissolved hydrogen (less aggressive). The proposed test matrix is given below along with the straining conditions:

Test type:	Constant extension rate tensile test
Sample design:	W tensile samples
Strain rate:	3 x 10^{-7} s^{-1}

The test matrix, Table 6, is designed to test the samples irradiated at 390, 407 and 427°C at a temperature of 400°C in both the SA and CW conditions in an inert environment and in two SCW environments; the reference, deaerated environment and an SCW environment containing additions of either O_2 or H_2. If the deaerated condition does not crack, then the more aggressive environment (containing O_2) will be selected and if it does, then the less aggressive (containing H_2) will be selected. The logic is to test the limits of the anticipated SCWR environment – high O_2 in the case of an environment in which recombination is difficult, and high H_2 environment in the case where H_2 additions are effective in suppressing oxygen.

Tests will also be conducted on the samples irradiated at 520°C. These tests will be conducted at 500°C in Ar, deaerated SCW and SCW containing either O_2 or H_2, as previously discussed.

Our objective is to obtain archive JPCA in order to establish baseline data on the SCC behavior of the unirradiated alloy. In this way, the test matrix as outlined will provide the following information:

- Effect of SCW on SCC of unirradiated JPCA
- Effect of irradiation on mechanical behavior of JPCA
- Effect of irradiation on SCC of JPCA in SCW at 400°C and at 500°C
- Effect of aggressiveness of SCW environment on JPCA at 400°C and 500°C
- Effect of dose on SCC in SCW at 400°C in deaerated SCW and in SCW containing either O_2 or H_2.

All SCC testing will be conducted in the supercritical water system in the Irradiated Materials Testing Laboratory at the University of Michigan that has been completed and has undergone final testing and check-out and is ready for neutron-irradiated samples.

Table 6. Test matrix for JPCA alloys irradiated in FFTF

Environment	Temperature (°C)	Sample #	Condition	Irrad. temp (°C)	Dose (dpa)
Ar – inert	400	2A/1A-1	SA	390	26.9
		2A/2E-1	SA	407	41.1
		2A/3D-2	SA	427	43.9
		2A/1A-1	CW	390	26.9
		2A/2E-1	CW	407	41.1
		2A/3D-2	CW	427	43.9
SCW - deaerated	400	2A/1A-1	SA	390	26.9
		2A/2E-1	SA	407	41.1
		2A/3D-2	SA	427	43.9
		2A/1A-1	CW	390	26.9
		2A/2E-1	CW	407	41.1
		2A/3D-2	CW	427	43.9
SCW – O_2 or H_2	400	2A/1A-1	SA	390	26.9
		2A/2E-1	SA	407	41.1
		2A/3D-2	SA	427	43.9
		2A/1A-1	CW	390	26.9
		2A/2E-1	CW	407	41.1
		2A/3D-2	CW	427	43.9
Ar – inert	500	2A/2D-2	SA	520	33.2
SCW – deaerated		2A/2D-2	SA	520	33.2
SCW - O_2 or H_2		2A/2D-2	SA	520	33.2

8. Arranging for Shipping and Receipt of the Samples

The following statement of work covers the shipping of samples from PNNL to the University of Michigan:

The University of Michigan, Ann Arbor has a contract with the DOE-NE GEN IV program to begin assessing the stress corrosion cracking resistance of candidate alloys for the GEN IV Super Critical Water Reactor concept. PNNL is in possession of some irradiated samples from the DOE Fusion program that the University of Michigan would like to test. PNNL has agreed to provide some of these samples to the University of Michigan. PNNL will also provide what information can be found on the composition and thermomechanical history of the samples. The University of Michigan will pay PNNL to ship the specimens to the University of Michigan, and the University of Michigan will assume all responsibility for the disposal of those specimens. The University of Michigan will also cover PNNL's cost to determine the composition and thermomechanical history of the samples. Samples should be ready to ship in early FY2006

9. Summary

Table 7 provides a report on the major milestones of this project. All milestones were completed and the facility is ready to accept irradiated samples and to begin testing in FY2006.

Table 7. Project Milestone Status

#	Milestone	Planned Completion Date	Actual Completion Date
1	Completion of the autoclave and SCC facility for testing neutron-irradiated samples	12/15/04	12/15/04
2	Testing of the operation of the facility (dry-run)	8/31/05	9/26/05
3	Benchmark Experiments in CERT and CGR modes	8/31/05	4/30/05
4	SEM installation	3/31/05	3/31/05
5	Operational check-out of the SEM	9/30/05	6/30/05
6	License Modification for the Phoenix Memorial Laboratory – determination of need and completion of any changes	6/30/05	7/31/05
7	Identification of the first batch of neutron irradiated samples for testing in FY2006	12/31/04	6/30/05
8	Arranging for shipping and receipt of the samples	7/31/05/05	9/20/05